Pflügers Arch - Eur J Physiol (1995) 430 : 283–292

ORIGINAL ARTICLE

Jürgen R. Schwarz · Gordon Reid · Hugh Bostock

Action potentials and membrane currents in the human node of Ranvier

Received: 3 August 1994 / Received after revision: 6 November 1994 / Accepted: 24 November 1994

Abstract Action potentials and membrane currents were recorded in single human myelinated nerve fibres under current- and voltage-clamp conditions at room temperature. Nerve material was obtained from patients undergoing nerve graft operations. Successful recordings were made in 11 nerve fibres. In Ringer's solution, large transient Na currents were recorded, which could be blocked completely with tetrodotoxin. Partial block of these currents with 3 nM tetrodotoxin was used to reduce the voltage-clamp error due to series resistance. Outward K currents were very small in intact nerve fibres, but had a large amplitude in fibres showing signs of paranodal demyelination. In isotonic KCl, the K current could be separated into three components: two fast components (K_{f1} and K_{f2}) and one slow component (K_s). Time constants and steady-state activation and inactivation of Na permeability and of fast and slow K conductance were measured within the potential range of −145 mV to +115 mV. From these parameters, the corresponding rate constants were calculated and a mathematical model based on the Frankenhaeuser–Huxley equations was derived. Calculated action potentials closely matched those recorded. Single calculated action potentials were little affected by removing the fast or slow K conductance, but the slow K conductance was required to limit the repetitive response of the model to prolonged stimulating currents.

Key words Myelinated nerve fibre · Action potential · Voltage clamp · Sodium current · Potassium currents

J. R. Schwarz (✉)
Physiologisches Institut, Universitätskrankenhaus Eppendorf, Martinistrasse 52, D–20246 Hamburg, Germany

G. Reid · H. Bostock
Sobell Department of Neurophysiology, Institute of Neurology, Queen Square, London WC1N 3BG, UK

Introduction

The first quantitative description of axonal membrane currents was made by Hodgkin and Huxley [21] for the giant axon of the squid. Later, Frankenhaeuser [17, 18] demonstrated that membrane currents measured in the frog node of Ranvier were similar to those of the squid axon and were composed of Na and K currents and a non-specific leakage current. Based on the quantitative analysis of these nodal currents, Frankenhaeuser and Huxley [19] were able to calculate action potentials which were similar to those measured.

Following a short description of action potentials and membrane currents in the rat [22], the first successful voltage-clamp experiments in mammalian nerve fibres were reported in the rabbit [13] and in the rat [9]. These studies clearly demonstrated that, in the mammalian myelinated nerve fibre, there is almost no nodal fast K current, and that activation of this current is therefore not necessary for action potential repolarization. In contrast, the slow K current which had previously been described in the frog node of Ranvier [16] is also present in the rat nodal membrane [28]. In rat, blocking this current with tetraethylammonium (TEA) produces prolonged repetitive activity in response to a long stimulus [2]. In frog nodes the slow K current has been modelled [16], and its effects on spike frequency adaptation have been described [1, 27], but no such model has previously been derived from measurements on mammalian nodes.

Because of the lack of human data, previous models of action potentials and slow excitability changes in human nerve fibres have been based on measurements from frog, rabbit or rat nodes, although extracellular recordings from human nerve in vivo have also been taken into account [5, 6]. K channel density differs substantially between frog and mammalian nodes [9, 13], and in rat fibres, K channel distribution changes with age [7]. Therefore, it has been open to question whether data from laboratory animals can provide a

satisfactory model of excitability in adult human axons. Rat nerve fibres accommodate more in response to step and ramp currents and discharge less readily during or after anoxia than do human axons in vivo; these differences could be reduced by treating the rat nerves with K channel blockers ([4] and our unpublished observations). Patch clamping of acutely demyelinated human axons [31] has shown that the main axonal channel types are similar to those in rat [30], but currents have not previously been recorded in intact human nodes of Ranvier.

The present study was undertaken to investigate the possible differences between action potentials and ionic currents in human and rat nodes of Ranvier, and to attempt to reproduce the electrical activity of human nodes using a model derived from the experimental data. We found that single myelinated nerve fibres could be isolated successfully from fresh human nerve, although the dissection was more difficult than in the rat, and that the node of Ranvier could be voltage and current-clamped. Part of the results have been published in abstract form [29, 33].

Materials and methods

Preparation and experimental procedure

Human peripheral nerve was obtained during post-traumatic graft or amputation surgery at the Royal National Orthopaedic Hospital, Stanmore, Middlesex, UK. Excess donor nerve, which would otherwise have been discarded, was collected at room temperature in tissue culture medium [Dulbecco's MEM/Ham's F12 with L-glutamine and 15 mM 4-(2-hydroxyethyl)-1-piperazineethanesulphonic acid (HEPES); Gibco, Paisley, Scotland, which had previously been equilibrated with a mixture of 95% O_2 and 5% CO_2. Specimens were transported to Queen Square and investigated within 2–6 h after removal from the patient. Nerves from four patients were used in this study. From one patient the ulnar nerve was obtained after amputation of the left arm because of severe neurofibromatosis. The other nerves used were excess graft material, comprising two sural nerves and one medial cutaneous nerve of the forearm.

The dissection procedure was modified from that described by Stämpfli and Hille [34]. The nerve was bathed in a trough filled with Ringer's solution. A nerve fascicle was isolated, desheathed and spread into a fan by simultaneously pulling apart the two sides of the nerve bundle with two dissection needles. This fan-forming procedure was continued until a single nerve fibre was isolated over a length of two internodes. Adhering nerve fibres and connective tissue fibres were cut off with a pair of iridectomy scissors. Care was taken that the nerve fibre to be isolated was never stretched and retained a wavy appearance throughout the dissection (Fig. 1). At this stage the nodes of Ranvier were barely visible. A narrow nodal gap usually appeared during the mounting of the fibre in the recording chamber. The procedure of mounting and recording was the same as that described by Stämpfli and Hille [34].

Action potentials and membrane currents were recorded with the current- and voltage-clamp method of Nonner [25]. The side pools of the experimental chamber were filled with axoplasmic solution (see below) and both internodes were cut. At the beginning of each experiment, the holding potential (E_H) was adjusted so that about 30% of the Na current was inactivated ($h_\infty = 0.7$). The potential at which $h_\infty = 0.7$ was estimated from two fibres as -84 mV and -86 mV, by superfusing the node with isotonic KCl and measuring the potential step required to reach the K equilibrium potential (E_K), assuming $E_K = 0$ mV. This value is more negative than those reported in rabbit (-80 mV, [13]) and rat (-80 mV, [9]; -78 mV, [23, 32]). In fibres in which E_H was not measured directly, the E value at which $h_\infty = 0.7$ was assumed to be -85 mV. Membrane current was recorded as the voltage drop across the internodal resistance, R_{ED} [25]. Based on unpublished rat data of B. Neumcke, J.R. Schwarz and R. Stämpfli, this resistance was assumed to be 14.4 ± 2.4 MΩ ($n = 13$), and this value was used to calculate absolute membrane currents.

Currents were filtered with a 4-pole Butterworth filter at 50 kHz and sampled at 100 kHz using pClamp (Axon Instruments, Foster City, Calif., USA) on an IBM PS/2 computer. In intact nerve fibres capacity transients had a duration of about 20 μs (two sample points); they were therefore not compensated by subtraction, but instead the points affected were deleted. In order to delay rundown [32], experiments were carried out at room temperature (25 ± 1 °C) or at 20 °C (the temperature of test solutions was controlled automatically by a cooler).

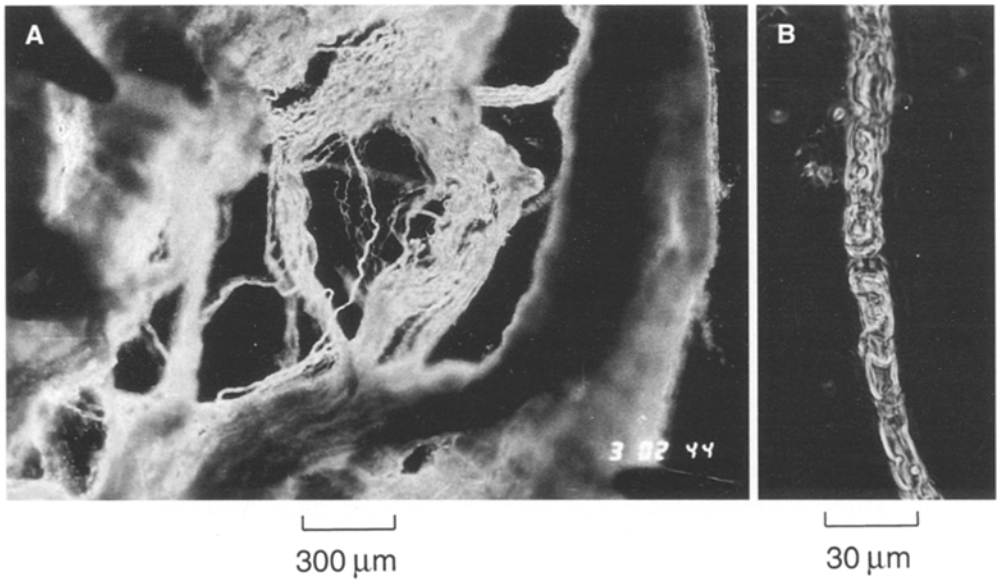

Fig. 1A, B Single myelinated nerve fibre isolated from a human sural nerve. **A** Overview of a fan (dark field); **B** single nerve fibre (phase contrast)

Solutions

The following solutions were used (in mM): Ringer's solution: NaCl 154, KCl 5.6, $CaCl_2$ 2.2. Isotonic KCl solution: KCl 155, $CaCl_2$ 2.2. Axoplasmic solution: KCl 155. Na-HEPES 4.54 and HEPES 5.46 were added to all solutions to give a pH of 7.4 at 25 °C. Tetrodotoxin (300 nM, TTX) was added to the external solutions for total block of Na currents and 3 nM TTX to block Na currents partially. K currents were blocked by 10 mM tetraethylammonium chloride (TEA) or 1 mM 4-aminopyridine (4-AP). TEA, 4-AP and TTX were purchased from Sigma; all the other substances were from Merck.

Results

Action potentials and repetitive activity

Action potentials and membrane currents were recorded in 11 fibres. Figure 2Aa shows an action potential recorded at 25 °C. Its amplitude was 116 mV and its duration near threshold potential was 1.4 ms, a duration which is longer than that of a rat action potential recorded at 20 °C [32]. In the other eight human nerve fibres where action potentials could be measured the amplitude was smaller and the threshold potential was higher (see Fig. 6D). These changes indicated that the fibres might have been damaged during dissection and mounting, leading to axoplasmic Na accumulation and to increased leakage current.

With a long-lasting depolarizing current stimulus, repetitive activity could be elicited in one fibre, see Fig. 2Ab. It can be seen that both the amplitude and the interspike interval increased during the train of action potentials. The frequency of the repetitive activity increased as the amplitude of the stimulating current was increased.

General description of membrane currents

Membrane currents recorded in a voltage-clamped human node of Ranvier are very similar to those recorded in rat [9, 28] or rabbit [13] nerve fibres. Figure 2Ba shows superimposed membrane currents elicited by depolarizing potential steps of increasing amplitude. The ionic currents consist of an early transient inward or outward current and a small steady-state outward current. In the presence of 300 nM TTX, the early transient current was totally blocked (Fig. 2Bb). By subtracting the unblocked currents from the total current, the TTX-sensitive current was obtained (Fig. 2Bc), which was assumed to be identical to the Na current. In the graph relating current to voltage (Fig. 2C), the peak Na current in the absence of TTX has its maximum amplitude near −40 mV and reverses its direction at E_{Na} = +25 mV (filled circles in Fig. 2C). In five nerve fibres E_{Na} ranged from 0 mV to +40 mV. In rat nerve fibres the mean E_{Na} was +72 mV [32]. The low value of E_{Na} in human nerve fibres is presumably caused by a higher axoplasmic Na concentration due to damage of the nodal membrane as mentioned above. The main part of the steady-state outward current is non-specific leakage current of undefined origin. There is only a very small outwardly rectifying K current, most of which could be blocked

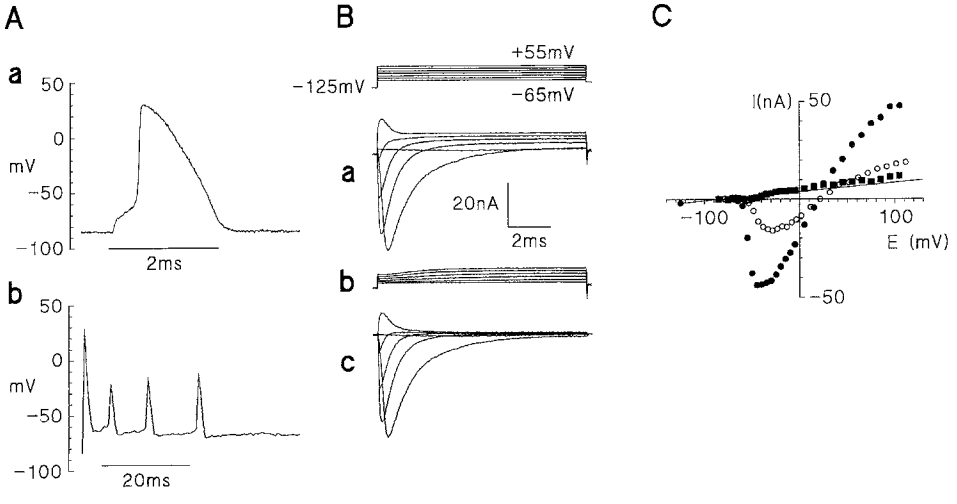

Fig. 2 Action potentials (**A**) and membrane currents (**B**) in a human node of Ranvier. **Aa** Action potential in a human node at 25 °C, in response to a 0.5-ms stimulus. **Ab** Repetitive activity recorded in response to a long-lasting depolarizing current. Same nerve fibre as in **Aa**. **B** Membrane currents in a different human node at 20 °C, in Ringer's solution (**a**) and in Ringer's solution containing 300 nM tetrodotoxin (TTX) (**b**). Test pulses of 10 ms duration to potentials between −65 mV and +55 mV were applied from a holding potential of −85 mV; traces recorded at 20-mV increments are shown. Each test pulse was preceded by a 50-ms pulse to −125 mV. Subtraction of membrane currents in **Bb** from those in **Ba** yielded the TTX-sensitive current (**Bc**). **C** Current-potential relation, peak transient current in Ringer's solution (*filled circles*) and in the presence of 3 nM TTX (*open circles*) as well as steady-state outward current (*squares*) from the same nerve fibre as shown in **B**. *Straight line* denotes leakage current extrapolated from the inward current recorded at −125 mV assuming a linear leakage conductance

with 4-AP (not shown). In three fibres, however, the K current was relatively large, presumably due to partial paranodal demyelination.

Na currents

In most fibres the peak Na current had a very steep potential dependence of activation within a small potential range (filled circles in Fig. 2C). The potential dependence became less steep and the maximum inward current shifted to more positive membrane potentials when the Na current was reduced by 3 nM TTX (open circles in Fig. 2C). This effect was interpreted as being due to a resistance in series with the nodal membrane, producing deviations between the clamp and the membrane potential which are proportional to the current amplitude [15, 24].

The time course of Na current activation at depolarizations more positive than −50 mV was determined from the time to peak of the activating Na current. Between −130 mV and −40 mV, the kinetics of Na current activation were measured using the time course of tail current deactivation recorded at these potentials after a constant 0.2-ms activating pulse (Fig. 3A).

The time course of Na current inactivation was determined from least-squares fits of the decay of Na currents recorded at potentials more positive than −50 mV. In many current traces, satisfactory fits of the membrane current decay were obtained only when two exponentials were used, whereas in Na currents reduced by TTX, a single exponential was sufficient. A similar observation has been reported in frog myelinated nerve fibres [3]. As in previous studies in frog [11] and rat [23, 32], the contribution of the slow component was potential dependent and was almost negligible at more positive potentials. Where possible, we fitted the Na current decay with only one time constant. These time constants were used for further quantitative analysis. At potentials < −50 mV, time constants of inactivation of Na permeability were determined with double-pulse protocols. An example of an experiment in which development of, and recovery from, inactivation of Na permeability at −89 mV was measured is shown in Fig. 3B.

The potential dependence of steady-state activation of Na permeability (m_∞) was determined from peak Na current amplitudes as described below. The potential dependence of steady-state inactivation of Na permeability (h_∞) was measured with a constant depolarizing test pulse preceded by 50-ms pre-pulses to potentials between −140 mV and 0 mV (Fig. 3Ca).

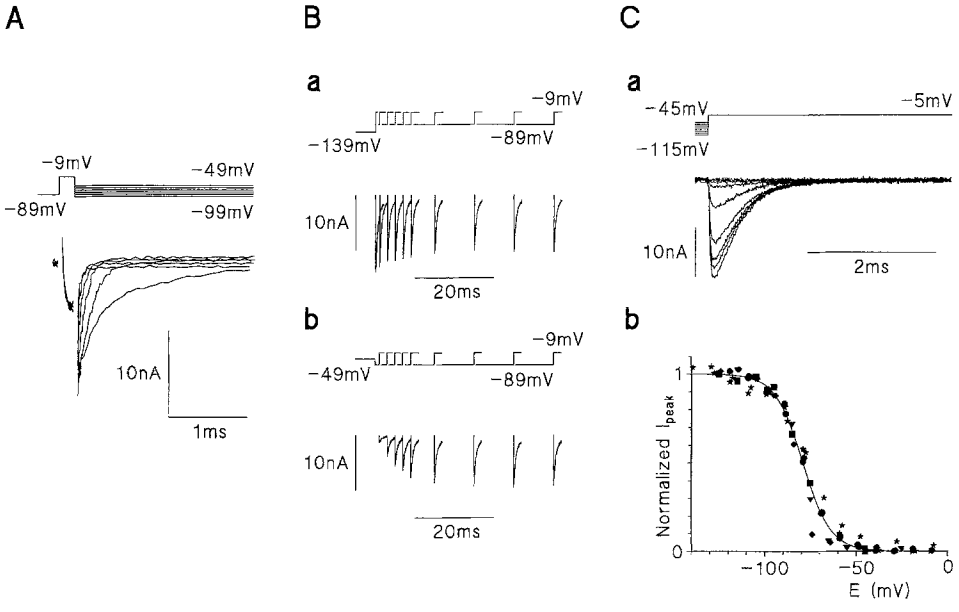

Fig. 3A–C Analysis of Na current activation and inactivation. **A** Na tail currents; membrane potential was stepped to potentials between −99 mV and −49 mV following a 0.2-ms pulse to −9 mV from a holding potential of −89 mV. **B** Membrane currents recorded to determine the time constant of development of (**a**) and recovery from (**b**) inactivation of Na permeability at −89 mV. **a** Inactivation of Na permeability was totally removed with a 50-ms hyperpolarization to −139 mV and the time course of development of inactivation was then traced with a test pulse to −9 mV after various time intervals. **b** Recovery from inactivation of Na permeability was studied with a similar double-pulse protocol, with the exception that Na permeability was totally inactivated with a 50-ms pulse to −49 mV before the conditioning pulse. Thereafter, recovery from inactivation was tested with a pulse to −9 mV after various time intervals. **C** Steady-state inactivation of the Na permeability; **a** Superimposed membrane currents elicited by a test pulse to −5 mV preceded by 50 ms pulses to membrane potentials between −115 mV and −45 mV in steps of 10 mV (see pulse protocol in the *top panel*). **b** Steady-state inactivation h_∞ of Na permeability determined in 4 human axons; normalized peak Na currents are plotted against pre-pulse potential. The continuous curve is the result of a least-squares fit to the measured points with the Boltzmann equation, $h_\infty = 1/\{1 + \exp[(E - E_h)/k]\}$ with the inflection potential $E_h = -79.1$ mV and the slope factor $k = 7.6$ mV

The normalized peak current amplitudes were plotted against pre-pulse potential and fitted with the Boltzmann equation (Fig. 3Cb). In some fibres, Na currents recorded during the test pulse continued to increase slightly as the pre-pulse potentials became more negative (not shown in Fig. 3Cb). This may be due to removal of slow inactivation of Na permeability at these potentials [8].

K currents

At nodes judged to be undamaged (because their capacity currents were fast and small), fast K currents were small in relation to the Na and leakage currents. In three fibres fast K currents were relatively large, but these fibres had slow capacity current components indicating partial paranodal demyelination, probably due to damage during the dissection procedure [12]. The maximum fast K conductance in Ringer's solution was 14, 16 and 36 nS in three apparently intact fibres and 138, 189 and 241 nS in three presumably demyelinated fibres.

As in frog [16] and rat nerve [28], the K current in human nerve fibres has both fast and slow components, which were analysed from membrane currents recorded in isotonic KCl, and by using longer pulses. Figure 4Aa shows recordings in an axon which had slow capacity transients, indicating probable partial demyelination. K currents were elicited with potential steps from –75 mV to +35 mV. Upon repolarization, tail currents were observed with slow and fast components. A large part of the fast K current component was blocked by 1 mM 4-AP (Fig. 4Ab). Subtracting the unblocked K current from the total currents, the 4-AP-sensitive current was obtained (Fig. 4Ba). Subtraction of the leakage current from the current in Fig. 4Ab yielded a current which consisted mainly of the slow K current (Fig. 4Bb). Fast and slow tail current components were separated by fitting a single exponential to the slow component and then subtracting it from the total tail current. The amplitude of the fast component is plotted against test-pulse potential in Fig. 4C. The potential dependence could not be described by a single Boltzmann function, suggesting that both fast (f_1 and f_2)K current components described in frog [16] and rat [14] may also be present in human nerve fibres. Results in this and two other axons indicated that the presumed f_1 component, activating within the range of –60 mV to –30 mV, is predominant in human nerve fibres, and the f_2 component activating at more positive potentials is small.

Slow K currents

Figure 4Bb shows that a K current is present in human nodes of Ranvier, which activates slowly during depolarizing potential steps and deactivates slowly upon repolarization to E_H. In all but one axon only depolarizing potential steps were applied in isotonic KCl. Experiments in frog [16] and rat [28] showed that at least 30% of the slow K conductance is already activated at the resting potential. This was confirmed in one human nerve fibre in which we applied hyperpolarizing potential steps in isotonic KCl. Figure 5Cb shows the potential dependence of slow K current activation in this axon (filled circles) and in three others, fitted as described below. In addition, the time constants of slow K current activation and deactivation are summarized in Fig. 5Cb. Most of the experiments were performed at 20 °C. In one recording of the slow K current made at 25 °C, the measured time constants were adjusted to 20 °C using a temperature coefficient,

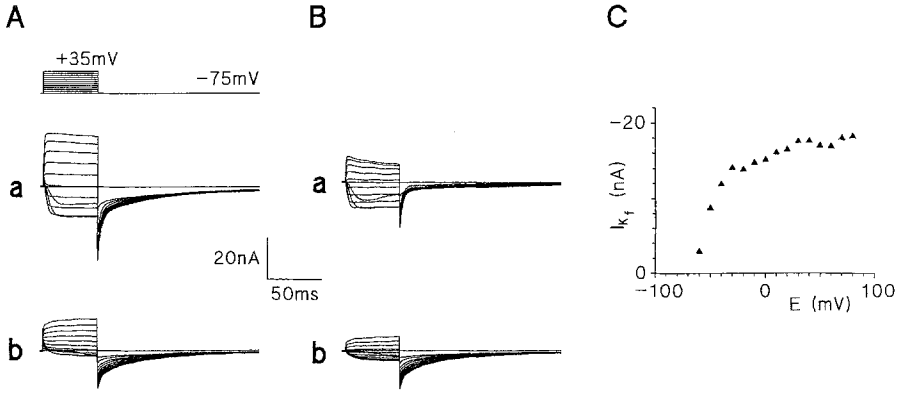

Fig. 4A–C Fast and slow K currents in a human axon with signs of partial paranodal demyelination. **Aa** Membrane currents recorded in isotonic KCl during 50-ms depolarizing potential steps from –75 mV to +35 mV in steps of 10 mV. **Ab** Same pulse protocol as in **Aa**, but in the presence of 1 mM 4-aminopyridine (4-AP). **B** K currents derived from the membrane currents shown in **A**. **Ba** 4-AP-sensitive current obtained by subtracting corresponding current traces shown in **Ab** from those in **Aa**. **Bb** Membrane currents shown in **Ab** corrected for leakage current. **C** Amplitude of fast K tail current component at –75 mV, plotted against the membrane potential of the test pulse. The amplitude of the fast component was obtained by fitting the sum of two exponential functions to the tail currents shown in **Aa**

Q_{10} of 3.0 (assuming it to be the same as for the fast K current in frog [20]).

Leakage current

Leakage current was assumed to be linear within the potential range investigated (see straight line in Fig. 2Ca). It could be measured directly in Ringer's solution using small test pulses in the vicinity of E_H, at which the amplitude of specific currents, e.g. of the slow K current, is negligible. The leakage conductance, which may represent an access conductance to the internodal axolemma rather than a nodal membrane conductance [2], tended to increase during an experiment and ranged from 30 nS to 110 nS; these values are larger than those reported in the rat (24 nS [32]).

Quantitative description of ionic currents

Na current

The quantitative analysis of Na permeability was made using membrane currents measured in two axons. In one of these axons the Na current amplitude had been decreased by 3 nM TTX to reduce the effect of the series resistance. Na currents during depolarizing pulses were assumed to follow the equation

$$I_{Na} = I'_{Na}[1 - \exp(-t/\tau_m)]^3 \exp(-t/\tau_h) \quad (1)$$

The parameters to be fitted were: I'_{Na}, amplitude of the Na current which would have been reached by full activation in the absence of inactivation; τ_m, τ_h, time constant of activation and inactivation, respectively, of Na permeability. The fits and further analysis were made as described by Schwarz and Eikhof [32], except that the time to peak of the Na current was used to obtain τ_m [23]. The rate constants $\alpha_m(E)$, $\beta_m(E)$, $\alpha_h(E)$ and $\beta_h(E)$ were derived from the steady-state parameters $m_\infty(E)$ and $h_\infty(E)$ and the time constants $\tau_m(E)$ and $\tau_h(E)$, and fitted using the equations given in the Appendix. The logarithm of the rate constants was used for the least-squares fits, in order to equalize the error in the fit over the potential range; otherwise the large values at extreme potentials would dominate the fit (Fig. 5A, B).

Fast K currents

Quantitative analysis of fast K currents was done using recordings from four nerve fibres. Because the presumed f_2 component was small, fast K currents were analysed in terms of a single component, which was

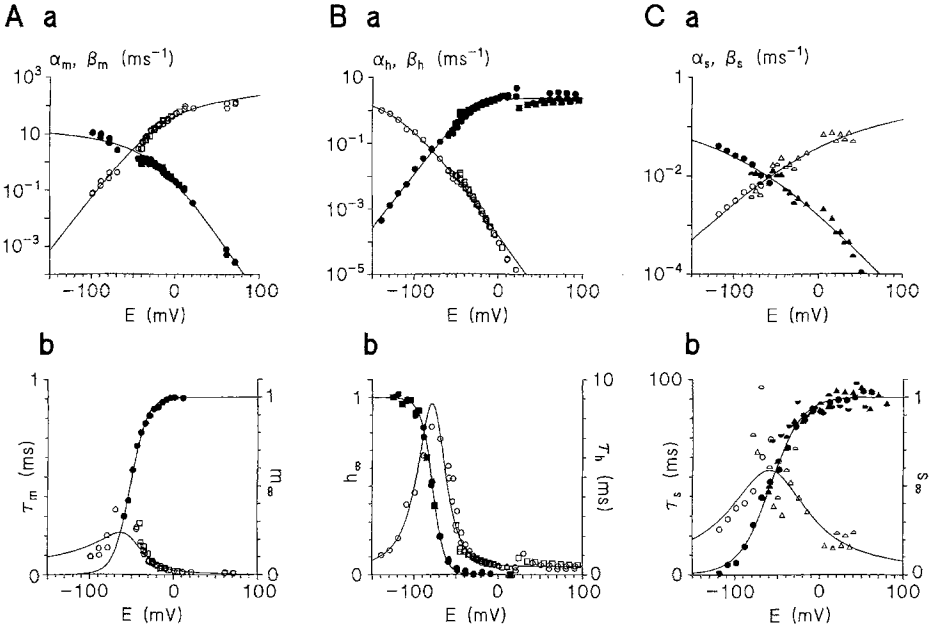

Fig. 5A–C Quantitative analysis of Na and slow K current kinetics. Rate constants of activation (**A**) and inactivation (**B**) of Na permeability, and activation (**C**) of slow K conductance in human node of Ranvier. The rate constants in the upper panels (**Aa**, **Ba** and **Ca**) were calculated from fits of the Boltzmann equation to measured values of m_∞, h_∞, and s_∞, and from the measured time constants τ_m, τ_h and τ_s, using the equations: $\alpha_m = m_\infty/\tau_m$, $\beta_m = (1 - m_\infty)/\tau_m$ (and similarly for h and s). *Open symbols* represent α_m, α_h and α_s and *filled symbols* β_m, β_h and β_s. Each *symbol type* represents a different axon. *Continuous lines* are the results of fits to the equations given in the Appendix. **Ab**, **Bb**, **Cb**, Time constants and steady-state values for activation and inactivation of Na permeability, and activation of slow K conductance, are plotted against membrane potential. *Filled symbols* represent steady-state values (m_∞, h_∞ and s_∞) and *open symbols* represent time constants (τ_m, τ_h and τ_s). *Symbol types* indicate the same axons as in **Aa**, **Ba** and **Ca**. *Continuous lines* were calculated from the fitted rate constants

assumed to be an ohmic conductance. The time constant τ_n of the fast K current was estimated from currents during depolarizing pulses in Ringer's solution (Fig. 2Bb), assuming that the current follows the equation:

$$I_{Kf} = I'_{Kf}[1 - \exp(-t/\tau_n)]^4 \quad (2)$$

Steady-state activation n_∞ was estimated from the 4th root of the amplitude of the fast component of tail currents in isotonic KCl (Fig. 4) and fitted with a Boltzmann function. The rate constants $\alpha_n(E)$ and $\beta_n(E)$ were derived as described for $\alpha_n(E)$ and $\beta_n(E)$.

Slow K current

Quantitative analysis of the slow K current was performed on recordings from four nerve fibres. The model of Dubois [16], with one open and one closed state of the channel, was used to describe the slow K current. However, the rate constants α_s and β_s were found to be better fitted with equations similar to those of the fast K current than those used by Dubois ([16]; see Appendix). The time constant τ_s was obtained at depolarized potentials by fitting the slow activation phase of K currents. At potentials near and negative to E_H, τ_s was obtained by fitting a single exponential to tail currents at these potentials following large depolarizations.

The steady-state value of the slow K conductance, s_∞, at potentials positive to E_H, was estimated from the amplitude of the slow tail current after long depolarizing pulses (> 500 ms). This gives a value of zero for the slow K conductance at E_H. Since part of the slow K current is already activated at E_H, the steady-state slow K conductance at potentials around and negative to E_H was determined in one experiment in which hyperpolarizing pulses were applied. In the three experiments in which no measurements at membrane potentials more negative than E_H were made, the proportion of the slow K conductance active at E_H was estimated by fitting a Boltzmann function with the inflection potential, $E_{0.5}$, fixed at -62 mV, a value obtained from the one experiment in which it was determined. Points from all four experiments were scaled from 0 to 1. The rate constants α_s and β_s were calculated as described for $\alpha_m(E)$ and $\beta_m(E)$.

Application of the human node model

Voltage-clamp currents

The currents produced by the model using the parameters given in the Appendix are shown in Fig. 6Ba and are compared with those measured (Fig. 6Aa). In addition, the current components are given separately, i.e. the TTX-sensitive current as obtained from the measured currents (Fig. 6Ac) is shown together with the modelled Na current (Fig. 6Bc), the current in Ringer's containing 300 nM TTX (Fig. 6Ab) together with the modelled K (fast and slow) and leakage currents (Fig. 6Bb).

Single action potentials

The action potential generated by the model using the data summarized in the Appendix (Fig 6C; smooth line) has an almost identical shape to that measured (Fig. 6C; noisy trace). When the fast K current is removed from the model, the effect on repolarization of the action potential is small (Fig 6C; dotted line). This lack of effect is similarly observed in other mammalian species when 4-AP is applied to the node, and suggests that nodal fast K channels play very little part in repolarization in human axons. The slow K current also has very little effect on the single action potential (not illustrated). Figure 6D shows that the same model can reproduce a smaller and slower action potential recorded from another node when allowance is made for a higher internal Na concentration, a larger leakage current and a hyperpolarizing holding current. It is clear from this recording that repolarization proceeds in two phases; modelling shows that this is due to inactivation (slow first phase) and deactivation (fast second phase) of Na permeability.

When a long depolarizing current stimulus is applied to the model, it simulates a train of action potentials (Fig. 6Ea) with characteristics similar to the trains of action potentials recorded in the axon shown in Fig. 2Ab. As in the measured repetitive activity, the amplitude of the second action potential is smaller than that of the first, and the remaining action potentials in the train have successively larger amplitudes. The interval between the action potentials increases until the repetitive activity dies out. The slow K current conductance shows a stepwise increase because activation becomes faster during each action potential. If the slow K current is removed from the model, a long depolarizing current stimulus produces sustained repetitive activity (Fig. 6Eb) which is similar to that recorded in rat spinal roots in the presence of TEA [2].

Discussion

This is the first report of successful recordings of action potentials and membrane currents in the human node of Ranvier. As in rat and rabbit, the predominant current in the intact human nodal membrane is the TTX-sensitive Na current. The fast K currents have a small amplitude in intact fibres and appear to have almost no effect on the shape of the single action potential. The slow K current, which was found to be present as

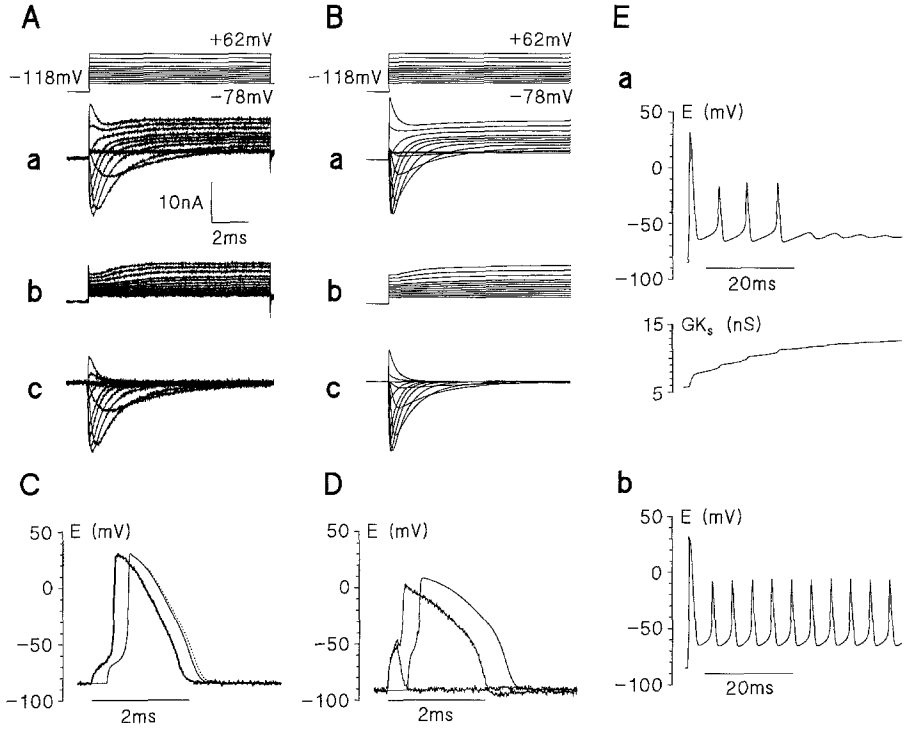

Fig. 6A–E Application of the human node model. **Aa** Superimposed membrane currents recorded in Ringer's solution containing 3 nM tetrodotoxin (TTX) with potential steps from −78 mV to +62 mV. Each depolarization was preceded by a 50-ms pre-pulse to −118 mV to remove steady-state inactivation of Na permeability. **Ab** Same experimental protocol as in **Aa**, but with 300 nM TTX added to the Ringer's solution. **Ac** TTX-sensitive current obtained by subtracting membrane currents shown in **Ab** from those in **Aa**. **Ba-c** Modelling of membrane currents shown in **Aa-c** with the equations given in the Appendix **C** Action potential as measured in a human node of Ranvier (same action potential as in **Fig. 2 Aa**) and computed action potentials with (*smooth line*) and without (*dotted line*) fast K conductance, calculated using the data in the Appendix, (25 °C). **D** Action potential and subthreshold local response measured in a different human node at 20°C, shown together with an action potential computed using the data in the Appendix modified as follows: $g_{leakage} = 40$ nS, $[Na^+]_i = 90$ mM, temperature 20 °C. A hyperpolarizing current was used in the recording to counteract the depolarization due to fibre rundown; + 0.3 nA of polarizing current was added to the model to simulate this current. Calculated action potentials in **C** and **D** are offset along the time axis for clarity. **Ea** Repetitive activity calculated from the data in the Appendix (*upper panel*) and time course of slow K conductance (*lower panel*). **Eb** Omission of slow K conductance from the model induces repetitive activity for the duration of the depolarizing current

a small amplitude current in Ringer's solution in all human axons investigated, appears to have important functional effects as previously inferred from in vivo measurements [4].

The quantitative analysis of the membrane currents, based on the equations given by Hodgkin and Huxley [21] for squid axons and by Frankenhaeuser and Huxley [19] for *Xenopus* nodes, yielded a model (Appendix 1) which reproduces the main characteristics of the recorded action potential. We used the Hodgkin–Huxley formulation, in preference to more complete models (e.g. [26]), to allow easy comparison with models decribed previously for other species and to minimize the number of parameters required to explain all the behaviour we had observed. Important parts of the model (e.g. the voltage dependence of activation of the Na current and of the slow K current negative to E_H) were based on recordings from only one fibre, but currents and action potentials recorded from other fibres could also be reproduced by adjusting the values of leakage conductance, internal Na concentration and series resistance. As in rat [32], the action potential of intact human nodes was closely approximated by equations for Na permeability and leakage conductance alone. The shape of the action potential remained essentially unchanged when fast or slow K conductances were added, except that on the time scale of the single action potential the slow K conductance behaves like a leakage conductance. This indicates that activation of the fast and slow K conductances is not involved in action potential repolarization. On a longer time scale, however, removal of the slow K conductance from the model induced an increase in repetitive firing, similar to that obtained by blockage of this current component by TEA in rat ventral root fibres [2].

Peak Na currents were consistently larger (range 40–50 nA) than has been reported previously in rat nodes (20–25 nA, [32]). However, this difference depends on the assumption that the axial resistances, through which the currents are delivered, are the same between species. Axial resistance measurements were not attempted in this study, since the method involves the destruction of the nodal membrane, and the

estimates obtained are very variable [13, 24]. Therefore, it is possible that the apparent larger size of the Na currents was due to a higher axial resistance of the human fibres. The human Na currents were not only higher in absolute terms compared with those in rat, but higher in relation to the amplitude of the leakage currents. A large Na permeability and a relatively small leakage conductance were also required to model the excitability of human nodes in vivo [5, 6] and could contribute to the greater tendency of human compared to rat fibres to discharge spontaneously and repetitively.

The deactivation of the slow K current at E_H values around -75 mV is faster in our experiments than has been reported to occur in rat fibres. This difference could not be explained by the effect of the pulse duration on the deactivation time constant described by Röper and Schwarz [28]. After 250-ms pulses to 0 mV, we recorded deactivation time constants of between 45 and 75 ms at between -70 mV and -80 mV (Fig. 5Cb), compared with around 160 ms in rat axons at -75 mV (see Fig. 3 of [28]). The possibility of a species difference is also supported by the observation that single K channels of the S (slow) type, which may correspond to the macroscopic slow K current, show faster deactivation in human axons (G.R., unpublished observations) than in rat axons [30].

In conclusion, our results show that human nodes of Ranvier contain a set of ionic channels which are very similar to those in rat and rabbit nodes and that a model comprising the Na permeability and the slow K and leakage conductances generates realistic action potentials and repetitive activity. As in other mammalian fibres, a fast K conductance appears to become important only with nodal widening. We have not attempted to model the contribution of internodal channels to fibre excitability (cf. [5]), but our new data on human Na and K channels provide the basis for constructing a quantitative model of the complete range of behaviours of human nerve fibres. The Na permeability may be larger at human than rat nodes, but further recordings with measurements of axial resistance are needed to establish this. In spite of the high susceptibility of the nodes to damage during dissection and isolation, voltage- and current-clamp studies in single human myelinated nerve fibres may help to clarify possible ion channel abnormalities in diseased human nerves (e.g. in diabetic or uraemic neuropathy; [10]).

Acknowledgements This study would have been impossible without the enthusiastic support of Mr. Rolfe Birch, Consultant Orthopaedic Surgeon, and colleagues at the Royal National Orthopaedic Hospital, Stanmore, Middlesex, UK, who provided us with excess nerve tissue. We thank the Deutsche Forschungsgemeinschaft for their financial support to J.R.S. (Schw 292), and the Medical Research Council and British Council for support to H.B. We would also like to thank Dr. C.K. Bauer and Dr. B.J. Corrette for reading the manuscript.

References

1. Awiszus F (1990) Effects of a slow potassium permeability on repetitive activity of the frog node of Ranvier. Biol Cybern 63: 155–159
2. Baker M, Bostock H, Grafe P, Martius P (1987) Function and distribution of three types of rectifying channel in rat spinal root myelinated axons. J Physiol (Lond) 383:45–67
3. Benoit E, Corbier A, Dubois J-M (1985) Evidence for two transient sodium currents in the frog node of Ranvier. J Physiol (Lond) 361:339–360
4. Bostock H, Baker M (1988) Evidence for two types of potassium channel in human motor axons in vivo. Brain Res 462: 354–358
5. Bostock H, Baker RM, Reid G (1991) Changes in excitability of human motor axons underlying post-ischaemic fasciculations: evidence for two stable states. J Physiol (Lond) 441: 537–557
6. Bostock H, Burke D, Hales JP (1994) Differences in behaviour of sensory and motor axons following release of ischaemia. Brain 117:225–234
7. Bowe CM, Kocsis JD, Waxman SG (1985) Differences between mammalian ventral and dorsal spinal roots in response to blockade of potassium channels during maturation. Proc R/Soc Lond [Biol] 224:355–366
8. Brismar T (1977) Slow mechanism for sodium permeability inactivation in myelinated nerve fibre of *Xenopus laevis*. J Physiol (Lond) 270:283–297
9. Brismar T (1980) Potential clamp analysis of membrane currents in rat myelinated nerve fibres. J Physiol (Lond) 298:171–184
10. Brismar T (1983) Nodal function of pathological nerve fibres. Experientia 39:946–953
11. Chiu SY (1977) Inactivation of sodium channels: second order kinetics in myelinated nerve. (Lond) J Physiol 273: 573–596
12. Chiu SY, Ritchie JM (1981) Evidence for the presence of potassium channels in the paranodal region of acutely demyelinated mammalian single nerve fibres. J Physiol (Lond) 313:415–437
13. Chiu SY, Ritchie JM, Rogart RB, Stagg D (1979) A quantitative description of membrane currents in rabbit myelinated nerve. J Physiol (Lond) 292:149–166
14. Corrette BJ, Repp H, Dreyer F, Schwarz JR (1991) Two types of fast K^+ channels in rat myelinated nerve fibres and their sensitivity to dendrotoxin. Pflügers Arch 418:408–416
15. Drouin H, Neumcke B (1974) Specific and unspecific charges at the sodium channel of the nerve membrane. Pflügers Arch 351:207–229
16. Dubois JM (1981) Evidence for the existence of three types of potassium channels in the frog Ranvier node membrane. J Physiol (Lond) 318:297–316
17. Frankenhaeuser B (1960) Quantitative description of sodium currents in myelinated nerve fibres of *Xenopus laevis*. J Physiol (Lond) 151:491–501
18. Frankenhaeuser B (1963) A quantitative description of potassium currents in myelinated nerve fibres of *Xenopus laevis*. J Physiol (Lond) 169:424–430
19. Frankenhaeuser B, Huxley AF (1964) The action potential in the myelinated nerve fibre of *Xenopus laevis* as computed on the basis of voltage-clamp data. J Physiol (Lond) 171:302–315
20. Frankenhaeuser B, Moore LE (1963) The effect of temperature on the sodium and potassium permeability changes in myelinated nerve fibres of *Xenopus laevis*. J Physiol (Lond) 169:431–437
21. Hodgkin AL, Huxley AF (1952) A quantitative description of membrane current and its application to conduction and excitation in nerve. J Physiol (Lond) 117:500–544
22. Horàckova M, Nonner W, Stämpfli R (1968) Action potentials and voltage-clamp currents of single rat Ranvier nodes. VIIth Proc Union Int Physiol Sci VII, XXIV Congress, Washington, D.C. USA, 1860, p 594

23. Neumcke B, Stämpfli R (1982) Sodium currents and sodium-current fluctuations in rat myelinated nerve fibres. J Physiol (Lond) 329:163–184
24. Neumcke B, Schwarz JR, Stämpfli R (1987) A comparison of sodium currents in rat and frog myelinated nerve: normal and modified sodium inactivation. J Physiol (Lond) 382:175–191
25. Nonner W (1969) A new voltage-clamp method for Ranvier nodes. Pflügers Arch 309:176–192
26. Patlak J (1991) Molecular kinetics of voltage dependent Na^+ channels. Physiol Rev 71:1047–1080
27. Poulter MO, Hashiguchi T, Padjen AL (1989) Dendrotoxin blocks accommodation in frog myelinated axons. J Neurophysiol 62:174–184
28. Röper J, Schwarz JR (1989) Heterogeneous distribution of fast and slow potassium channels in myelinated rat nerve fibres. J Physiol (Lond) 416:93–110
29. Reid G, Bostock H, Schwarz JR (1993) Quantitative description of action potentials and membrane currents in human node of Ranvier. J Physiol (Lond) 467:247P
30. Safronov BV, Kampe K, Vogel W (1993) Single voltage-dependent potassium channels in rat peripheral nerve membrane. J Physiol (Lond) 460:675–691
31. Scholz A, Reid G, Vogel W, Bostock H (1993) Ion channels in human axons. J Neurophysiol 70:1274–1279
32. Schwarz JR, Eikhof G (1987) Na currents and action potentials in rat myelinated nerve fibres at 20 and 37 °C. Pflügers Arch 409:569–577
33. Schwarz JR, Reid G, Bostock H (1993) Action potentials and membrane currents in single human myelinated nerve fibres. Pflügers Arch 422 [Suppl 1]: R18
34. Stämpfli R, Hille B (1976) Electrophysiology of the peripheral myelinated nerve. In: Llinàs R, Precht W (eds) Frog neurobiology. Springer, Berlin, Heidelberg, New York, pp 3–32

Appendix

Equations and data used to model membrane currents and action potentials of human node of Ranvier.

Equations

Voltage clamp: $E = E_{command} - I_{total} R_{series}$
Current clamp: $dE/dt = -(I_{total} + I_{stimulus} + I_{polarizing})/C_{nodal}$
(normally R_{series} and $I_{polarising}$ are zero, unless specified in the text or figure legends)

$$I_{total} = I_{Na} + I_{Kf} + I_{Ks} + I_{leakage}$$

$$I_{Na} = m^3 h P_{Na} \frac{EF^2}{RT} \frac{[Na]_0 - [Na]_i \exp(EF/RT)}{1 - \exp(EF/RT)}$$

$$I_{Kf} = n^4 g_{Kf} (E - E_K)$$

$$I_{Ks} = s g_{Ks} (E - E_K)$$

$$I_{leakage} = g_{leakage} (E - E_{leakage})$$

$dm/dt = \alpha_m (1-m) + \beta_m m$ (and similarly for h, n and s) Integration of differential equations was performed by the Euler method. E is potential, I is current, R is resistance, C is capacitance, I_{Na}, I_{Kf} , I_{Ks} are Na, fast K and slow K currents respectively, m, n and s are activation parameters, h is an inactivation parameter, P_{Na} is Na permeability, g_{Kf}, g_{Ks} and $g_{leakage}$ are fast K, slow K and leakage conductances respectively, α and β are rate constants.

Parameters used for calculation

$E_{resting} = -84$ mV; $P_{Na} = 3.52 \times 10^{-9}$ cm$^3 \cdot$ s^{-1}; $[Na]_o = 154$ mM; $[Na]_i = 35$ mM; $[K]_o = 5.6$ mM; $[K]_i = 155$ mM; $E_K = -84$ mV; $g_{Kf} = 15$ nS; $g_{Ks} = 30$ nS; $g_{leakage} = 30$ nS; $E_{leakage} = -84$ mV; $C_{nodal} = 1.4$pF [a].

Voltage dependence of the rate constants α and β

Table 1 The constants A, B and C below were derived from the following equations [19] (valid at 20 °C):

α_m, α_n, $\alpha_s = A(E-B)/\{1-\exp[(B-E)/C]\}$

α_h, β_m, β_n, β_s, $= A(B-E)/\{1-\exp[(E-B)/C]\}$

$\beta_h = A/\{1+\exp[(B-E)/C]\}$

Rate constant	Constants		
	A (ms^{-1})	B (mV)	C (mV)
α_m	1.86	−18.4	10.3
β_m	0.0860	−22.7	9.16
α_h	0.0336	−111.0	11.0
β_h	2.30	−28.8	13.4
α_n	0.00798	−93.2	1.10
β_n	0.0142	−76.0	10.5
α_s	0.00122	−12.5	23.6
β_s	0.000739	−80.1	21.8

If the model was to be run at a temperature other than 20 °C, the rate constants were modified using the following Q_{10} values:

Table 2 Calculation of rate constants at temperatures other than 20 °C.

Rate Constant	Q_{10}	Source
α_m, β_m	2.2	[32]
α_h, β_h	2.9	[32]
α_n, β_n	3.0	[20]
α_s, β_s	3.0	